Proceedings of the 2018 IEEE/ASME International
Conference on Advanced Intelligent Mechatronics (AIM),
Auckland, New Zealand, July 9-12, 2018

A Single-Actuator Gripper with a Working Mode Switching Mechanism for Grasping and Rolling Manipulation

Huan Liu, *Student Member, IEEE,* Zhaoyu Zhang, Tianlai Dong,
Xiangyang Zhu*, Member, IEEE,* and Kai Xu*, *Member, IEEE*

***Abstract*—This paper presents a three-fingered gripper with a working mode switching mechanism for both grasping and rolling manipulation tasks, actuated by only one motor. A newly proposed Continuum Differential Mechanism (CDM) was utilized with an underactuated finger design to generate adaptive grasps. A switching mechanism was designed to change the gripper's working mode between grasping and rolling manipulation under the actuation of the same motor. Besides being expected to grasp various objects, the gripper can roll grasped objects with its two fingers, utilizing the CDM's elasticity, in the rolling manipulation mode. Experimental results verified that the gripper can adaptively grasp various objects in the grasping mode and can also perform in-hand rolling tasks using two of its fingers in the manipulation mode, demonstrating the effectiveness of the proposed idea.**

I. Introduction

In pick-and-place tasks across many industries, reorienting the picked objects before placing them down is a highly demanded movement. Many pick-and-place robots incorporate a fourth DoF (Degree of Freedom) for this purpose (e.g., the distal revolute joint of a SCARA robot or a DELTA robot). If a gripper can achieve both grasping and rolling manipulation, it can potentially save the fourth motor from a pick-and-place robot.

For the reason mentioned above, several robotic grippers have been proposed for both grasping and in-hand manipulation, via the use of additional independently driven mechanisms at their phalanges or fingertips. After grasping an object, these grippers reposition or reorient the object within the gripper with the additional actuators. For example, the turntables were used at the fingertips [1-3], while other approaches were also attempted, including the use of the plain belts at the phalange surfaces [4], the linear motors at the distal phalanges [5], and the translatable and rotatable stick-shaped fingers actuated by two addition motors [6]. Although these finger designs did enhance the grippers' manipulation dexterity, concerns may still stem from the additional cost of the extra actuators and the increased structural complexity of the fingers.

This work was supported in part by the National Natural Science Foundation of China (Grant No. 51722507, Grant No. 51435010 and Grant No. 91648103), and in part by National Key R&D Program of China (Grant No. 2017YFC0110800).

Huan Liu, Zhaoyu Zhang and Tianlai Dong are with the UM-SJTU Joint Institute, Shanghai Jiao Tong University, Shanghai, China (e-mails: hzauliuhuan@gmail.com, zhangzhaoyu@sjtu.edu.cn and 5123709073@sjtu.edu.cn).

Kai Xu and Xiangyang Zhu are with the State Key Laboratory of Mechanical System and Vibration, School of Mechanical Engineering, Shanghai Jiao Tong University, Shanghai, China (asterisk indicates the corresponding author, phone: +86-21-34206547; emails: k.xu@sjtu.edu.cn and mexyzhu@sjtu.edu.cn).

It is also possible to utilize extrinsic resources, such as motion dynamics, gravity, or external disturbance, to realize grasping as well as manipulation. The examples include the use of motion dynamics for re-grasping [7], prehensile pushing [8], controlled slipping under gravity [9] and dynamic in-hand sliding [10]. Although this approach alleviates the need for complex robotic hand designs, it brings challenges to the modeling and control of the hand-object system.

Underactuated hands are often designed for grasping. Recently, a framework of performing in-hand manipulation by utilizing the elasticity of underactuated fingers extended the functionality of underactuated hands [11]. Several grippers with in-hand manipulation capabilities have been introduced, including the iRobot-Harvard-Yale (iHY) hand [12], the GR2 gripper [13, 14], the caging manipulation gripper [15] and the Reflex hand (RightHand Robotics, Inc.) [16].

It can be seen from the previous examples that underactuated hand can perform grasping as well as in-hand manipulation if well designed. Following this philosophy, this paper presents a three-fingered underactuated gripper for grasping and rolling manipulation tasks, using only one motor, as shown in Fig. 1.

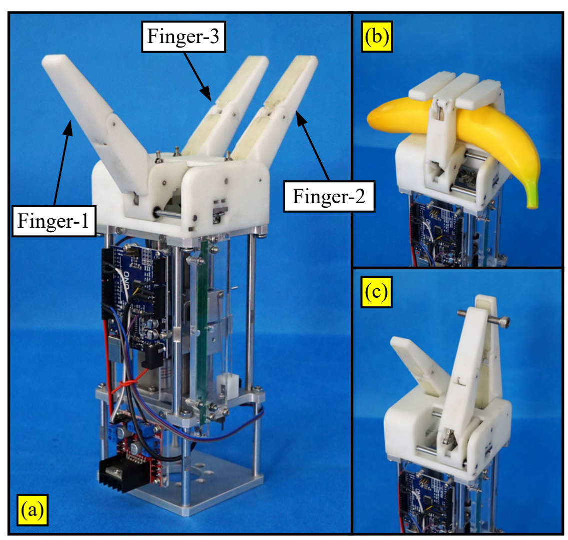

Fig. 1. The proposed gripper: (a) an overview, (b) the gripper in the grasping mode and (c) in the manipulation mode.

A newly proposed Continuum Differential Mechanism

(CDM) [17] was utilized together with an conventional underactuated finger design from [18] to generate adaptive grasps. A working mode switching mechanism was designed to change the gripper's working mode between grasping as in Fig. 1(b) and rolling manipulation as in Fig. 1(c). The gripper is actuated by a single motor. In the rolling manipulation mode in which the Finger-1 opposes the Finger-2, the gripper can roll grasped objects utilizing the CDM's elasticity. Design details and the analysis for the in-hand rolling manipulation are presented. Various experiments were conducted to show the grasping and rolling manipulation capabilities of the gripper.

This paper is organized as follows. In Section II, design details of the gripper are presented. Section III describes the formulation of the two-fingered rolling manipulation. Experimental characterizations are reported in Section IV with the conclusions and discussions summarized in Section V.

II. Design Descriptions of The Gripper

This section presents the gripper's design descriptions. The actuation strategy is first summarized in Section II.A. The descriptions of the underactuated finger, the CDM and the mode switching mechanism are presented in Section II.B, Section II.C and Section II.D, respectively. The control hardware is elaborated in Section II.E.

A. Actuation Strategy

The actuation strategy of the gripper is explained as follows, referring to Fig. 2. Since there is only one motor in the gripper, the two rotation directions of the motor are utilized to actuate the finger flexion and the mode-switching motion, respectively. The finger extension is realized by the torsional springs installed at the finger joints

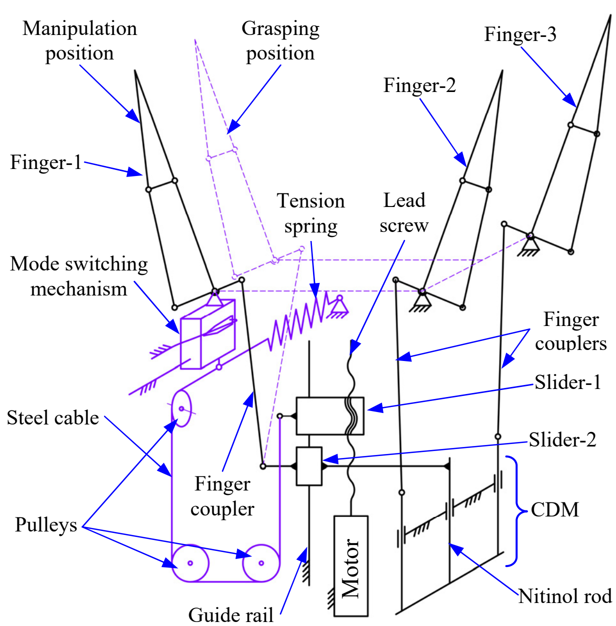

Fig. 2. Actuation strategy of the gripper.

The motor drives a lead screw, which actuates the Slider-1 to move up and down along a guide rail. A stainless-steel cable is anchored on the Slider-1 and routed to the movable base of the Finger-1.

The Slider-2 also translates along the same guide rail as the Slider-1. A coupler (the finger coupler in Fig. 2) connects the Slider-2 and the Finger-1 such that the Slider-2 drives the Finger-1. A nitinol rod is fixed on the Slider-2 and it is used as the input backbone of a CDM. The CDM generates two differential outputs which drive the Finger-2 and Finger-3 via two more finger couplers.

The Finger-1 is mounted on the mode switching mechanism such that the Finger-1 can be repositioned to either the grasping or the rolling manipulation position.

When the Slider-1 moves downward, it pushes the Slider-2 downward accordingly. As the Finger-1 is pulled to close, the Finger-2 and the Finger-3 are driven by the two differential outputs of the CDM. The steel cable, which is anchored on the Slider-1, will be slack and the mode switching mechanism does not change the position of the Finger-1.

When the Slider-1 moves upward, the Slider-2 firstly moves accordingly because the torsional springs at the finger joints restore the fingers to the extended positions. As the Slider-1 moves further, the cable will pull the mode switching mechanism via the steel cable and switch the position of the Finger-1. Therefore, the gripper can switch between the grasping mode and the manipulation mode, as shown in Fig. 1(b and c), respectively.

B. Finger Design

The gripper has three identical fingers and each finger has two revolute joints driven by a finger coupler made of nitinol rod with a diameter of 1.2 mm.

Take the Finger-1 as an example, flexion of the proximal and the distal joints are coupled through a joint coupler, as shown in Fig. 3. A torsional spring is installed at the distal joint while another torsional spring with lower stiffness is installed at the proximal joint.

When the crank is rotated by pulling the finger coupler, the proximal joint will rotate first. Then if the proximal phalange encounters an object, continuing to pull the finger coupler will close the distal joint, thus conformal finger configuration is formed. This underactuated finger design is adopted from the prominent design in [18].

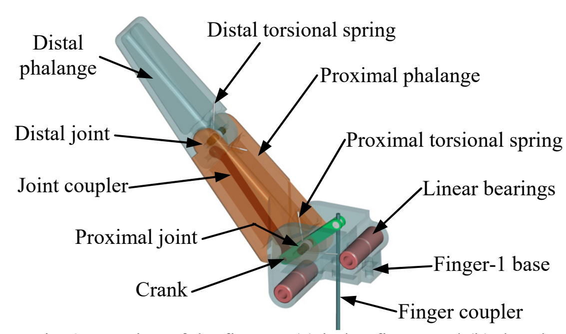

Fig. 3. Design of the fingers: (a) index finger and (b) thumb

The Finger-2 and Finger-3 are mounted on the palm, while the Finger-1 is installed on the mode switching mechanism which repositions the Finger-1 to either the grasping or the rolling manipulation position.

C. *Continuum Differential Mechanism*

Various differential mechanisms can be found in a wide spectrum of mechanical systems. Differential mechanisms were recently categorized as KDM (Kinematic Differential Mechanism) and CDM (Continuum Differential Mechanism) in [17], extending the categorization in [19].

A KDM generates differential outputs via the relative motions of its kinematic pairs, while a CDM generates differential outputs via the deformation or redistribution of its structure and/or material. KDMs used in robotic hand designs include: i) the pulley-based form [20], ii) the linkage-based form [21], and iii) the gear-based form [22]. The CDMs used in robotic hand designs include the fluidic T-pipe-based design [23] and the CDM-based design [24].

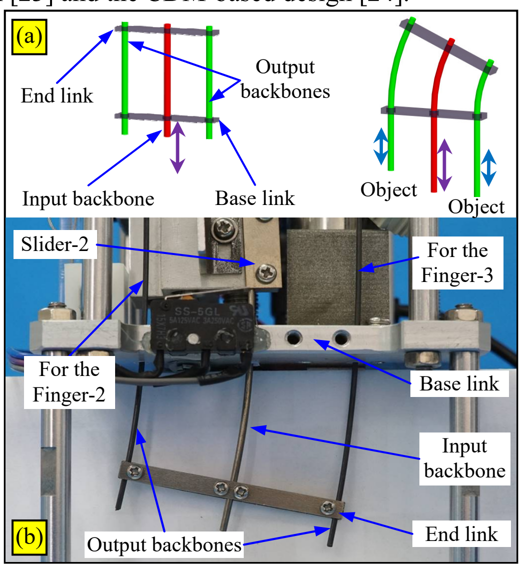

Fig. 4. The CDM: (a) schematic and (b) the implementation in the gripper

The working principle of a planar CDM is explained as in Fig. 4(a). The CDM consists of a base link, an end link, an input and two output backbones. All the backbones are made from super-elastic nitinol rods. They are attached to the end link and can slide in the holes in the base link. A force acts on the input backbone, while the two output backbones are connected to two external objects. If the object on the left is subject to a bigger resistance, continuously driving the input backbone will bend all the backbones to the right then differential outputs will be generated. The CDM can provide pushing and pulling outputs, since the backbones can be pushed or pulled.

The CDM is advantageous in terms of structural simplicity, design compactness and light weight. Moreover, it does not require any tension-keeping components which are essential for tendon-based differential mechanisms, due to the backbones' intrinsic elasticity.

A planar CDM driven by the Slider-2 is integrated in the gripper's base, as shown in Fig. 4(b). The Finger-2 and Finger-3 is driven by the two outputs of the CDM via two finger couplers, while the Finger-1 is directly driven by the Slider-2 via another finger coupler.

In the presented design, the output backbones are made from Ø1.2 mm nitinol rods. The input backbone is made from Ø1.5 mm nitinol rod since it undergoes compressive force. The distance between the two output backbones is 45 mm, which is determined according to the separation between the Finger-2 and the Finger-3.

D. *Mode Switching Mechanism*

The working mode switching mechanism is designed to switch the gripper between the grasping mode and the rolling manipulation mode by repositioning the Finger-1.

The base of the Finger-1, with a one-way plate cam mounted, translates along the guide shafts installed in the palm, as shown in Fig. 5(a). A hook mounted on the palm at one end has the other end travel inside the groove of the plate cam. The hook can only travel in one direction in the groove due to the height difference inside the groove, as shown in Fig. 5(b).

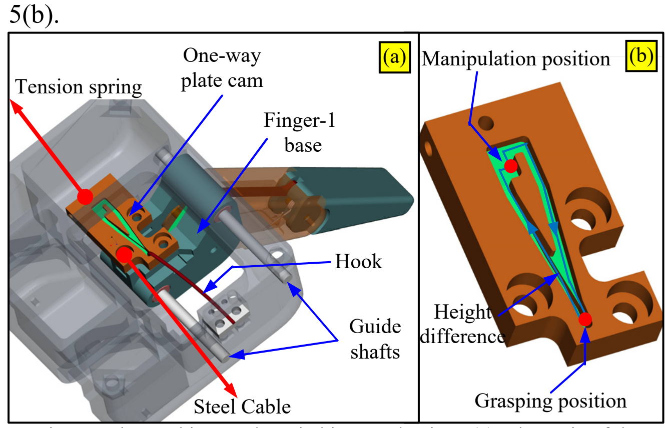

Fig. 5. The working mode switching mechanism: (a) schematic of the mechanism and (b) detail of the one-way plate cam

The steel cable, which is attached to the plate cam, is routed to the Slider-1 through multiple pulleys. The plate cam is pulled by a tension spring, as shown in Fig. 2.

Initially the hook is at the grasping position as in Fig. 5(b) (the gripper is in the grasping mode). If the Slider-1 pulls the plate cam via the cable, the hook travels in the groove of the plate cam from the grasping position to the manipulation position, as shown in Fig. 5(b). When the pulling force from the Slider-1 is removed and the cable is slack, the hook holds the plate cam at the manipulation position (a.k.a., the gripper stays in the manipulation mode). As the Slider-1 pulls the cable again, the hook will travel back to the grasping position so that the gripper is switched back to the grasping mode.

The hook holds the plate cam at the grasping or the manipulation position under the tension from the spring. The cable can be slack and the Slider-1 is free to move downward to drive the fingers' flexion. In this way, the finger flexion and the mode switching are enabled by a single actuator.

E. *Control and Actuation Hardware*

The control and actuation hardware using commercially available electronic components was designed as shown in Fig. 6.

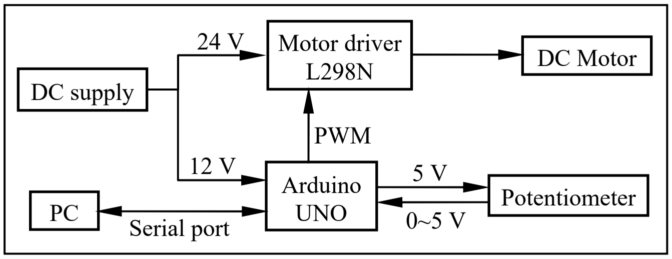

Fig. 6. Schematic of the control and actuation hardware

The hardware is powered by an external DC supply. The Arduino UNO as a controller receives control commands from a PC via its serial port. It reads the position of the Slider-1 from a linear potentiometer (KTL-100L from XiYu Electronic Co., China). The Arduino UNO controls the DC motor (Maxon DCX22L 24V with GPX22A 3.9:1 gearbox) via a L298N motor diver.

III. Manipulation Kinematics

This section elaborates the analysis on the two-fingered rolling manipulation of the gripper.

In the manipulation mode, an object is pinched by the distal phalanges of the Finger-1 and the Finger-2, as shown in Fig. 1(c). Because of the fingers' specific underactuated design, each finger is modeled as one link as shown in Fig. 7, where the distal finger joint is extended.

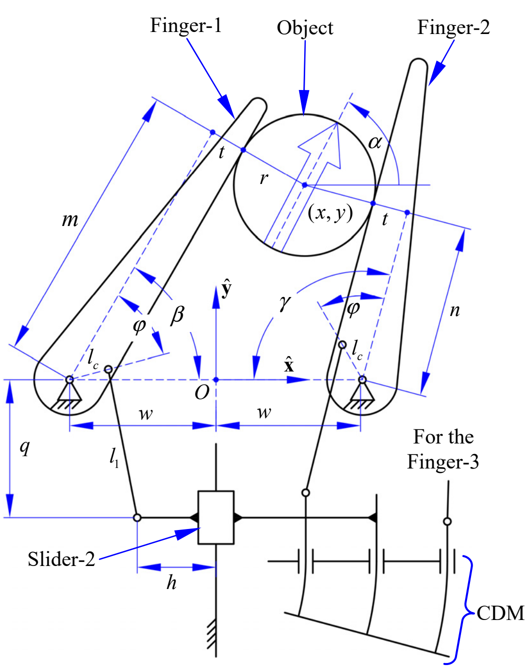

Fig. 7. Kinematics of the gripper manipulating a cylindrical object

The Finger-2 is connected to an output backbone of the compliant CDM and the input backbone is thicker than the output one. Once the gripper pinches an object in the manipulation mode, continuing to push the Slider-1 will hence drive the Finger-1 to flex more at its proximal joint. The Finger-2 is then pushed to extend at the proximal joint (the Finger-2 opens).

A cylindrical object with a diameter of r is modeled in this analysis for simplicity. As shown in Fig. 7, the configurations of the fingers and the object are related by Eq. (1) and Eq. (2) for the Finger-1 and Finger-2 respectively:

$$\begin{pmatrix} -w \\ 0 \end{pmatrix} + m \begin{pmatrix} \cos\beta \\ \sin\beta \end{pmatrix} + (t+r) \begin{pmatrix} \sin\beta \\ -\cos\beta \end{pmatrix} = \begin{pmatrix} x \\ y \end{pmatrix} \tag{1}$$

$$\begin{pmatrix} w \\ 0 \end{pmatrix} + n \begin{pmatrix} -\cos\gamma \\ \sin\gamma \end{pmatrix} + (t+r) \begin{pmatrix} -\sin\gamma \\ -\cos\gamma \end{pmatrix} = \begin{pmatrix} x \\ y \end{pmatrix} \tag{2}$$

Where w is half of the finger separation between the Finger-1 and the Finger-2, m and n is the distance between the proximal joint and the contact point along the length of the Finger-1 and the Finger-2 respectively, t is the thickness of the finger on the finger pad side, β and γ is the joint angle of the Finger-1 and the Finger-2 respectively.

The Finger-1 is driven by the Slider-2 via a finger coupler with a length of l_1. Pushing the Slider-2 downward drives the Finger-1 to flex satisfying Eq. (3):

$$l_1 = \left\| \begin{pmatrix} -w \\ 0 \end{pmatrix} + l_c \begin{pmatrix} \cos(\beta-\varphi) \\ \sin(\beta-\varphi) \end{pmatrix} - \begin{pmatrix} -h \\ -q \end{pmatrix} \right\| \tag{3}$$

Where l_c is the length of the crank of the fingers, φ is the angle for specifying the connection position of the finger crank, h is the length of the arm on the Slider-2 that drives the Finger-1, and q is the actuation of the Slider-2.

An initial configuration of the object is assumed to be (x_0, y_0, α_0) with respect to the coordinate $\{\hat{\mathbf{x}}, \hat{\mathbf{y}}\}$ attached to the palm. The gripper's configuration (β_0, γ_0, m_0 and n_0) can be solved by substituting (x_0, y_0) to Eq. (1) and Eq. (2). Similarly, q_0, which is the initial position of the Slider-2, can be obtained by substituting β_0 to Eq. (3).

When the object is rolled between the two fingers without slippage, the variations of the contact points along the phalanges and the rolled angle of the object satisfy Eq. (4):

$$\begin{cases} m = m_0 + \Delta\alpha_\beta r \\ n = n_0 - \Delta\alpha_\gamma r \end{cases} \tag{4}$$

Where $\Delta\alpha_\beta = \Delta\alpha - \Delta\beta$ and $\Delta\alpha_r = \Delta\alpha + \Delta\gamma$ is the right-handed rotation angle of the object with respect to the Finger-1 and the Finger-2, respectively.

When the Slider-2 is actuated with an incremental actuation Δq from the initial configuration, β can be first solve by Eq. (3). Then, the object's configuration (x, y, α) can be solved by the gripper-object geometry in Eq. (1) and Eq. (2) and the rolling constrains in Eq. (4).

The rotation angle $\Delta\alpha$ of multiple cylinders with different diameters (5mm, 10mm, 20mm and 30mm, respectively) were simulated and plotted alongside the experimental results in Fig. 9(c), using the structural parameters listed in Table I and the measured configurations of the objects in the experimental characterizations.

TABLE I. Structural Parameters of the Proposed Gripper

$\varphi = 85^\circ$	$h = 18mm$
$w = 27.5mm$	$t = 7mm$
$l_1 = 112mm$	$l_c = 15mm$

IV. Experimental Characterizations

In order to evaluate the effectiveness of the proposed gripper for both grasping and manipulating objects, two sets of experimental characterizations were conducted.

A. *Grasping Capabilities*

To evaluate the gripper's grasping capability, the gripper was commanded to grasp various objects. Some of the objects used are from the YCB object set [25].

Since there is no tactile sensor on the fingers, a simple stall detection algorithm is implemented to prevent the motor from overheating as follows. When the gripper is commanded to close, if the readout of the potentiometer stays unchanged (within a fluctuation threshold) for more than 300 ms, the gripper is determined as holding an object. Then, the power to the motor is switched off. Since the lead screw is not backdrivable, the grasp is maintained.

The gripper can perform various grasps including power grasp and pinch, as shown in Fig. 8(a) and (b) respectively.

For power grasps shown in Fig. 8(a), once the proximal phalanges were stopped by the object, the distal phalanges continued to flex, leading to conforming grasps.

For the pinches shown in Fig. 8(b), the gripper grasped the object only by the distal phalanges. Because of the specific underactuated finger design, the distal joints of the fingers were extended.

Because of the differential output generated by the CDM, the finger can adapt to different objects. For example, as the gripper pinched a foam plate, which was intentionally cut to the irregular shape shown in the right-lower corner in Fig 8, the backbones of the CDM were bent to the configuration shown in Fig. 4(b) for these differential outputs.

A multimedia extension for grasp demonstrations is also included.

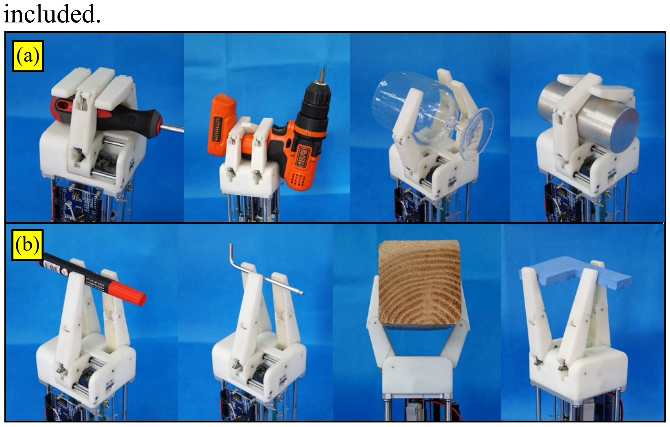

Fig. 8. Grasping experiments: (a) power grasps and (b) pinches

B. *Manipulation Performance*

The cylindrical objects as in Fig. 9(a) made by 3D printing with the diameters of 5 mm, 10 mm, 20 mm and 30 mm respectively, were used to verify the rolling manipulation performance of the gripper.

The configurations of the cylinders were measured using the experimental setup shown in Fig. 9(b). Two markers were attached to the palm of the gripper and each cylindrical object. An optical tracker (MicronTracker SX60, Claron Technology Inc.) was used to measure the positions and orientations of the markers. Then the configuration of the object with respect to the palm can be calculated.

The gripper was switched to the rolling manipulation mode and was commanded to pinch a cylinder using the Finger-1 and the Finger-2. Then the gripper was actuated in increments of 0.4 mm until the motor stalled. The configurations of the palm and the object were recorded. Then, the gripper was returned to its initial configuration. The quantifications were repeated for three times for each object. The average of the measured $\Delta\alpha$ was plotted in Fig 9(c). The average of the total measured rolling ranges of each cylindrical object is listed in Table II.

Using the measured initial configurations of the objects, $\Delta\alpha$ is also simulated via the analysis presented in Section III. The simulated results are plotted in Fig. 9(c) together with the measurements for comparison.

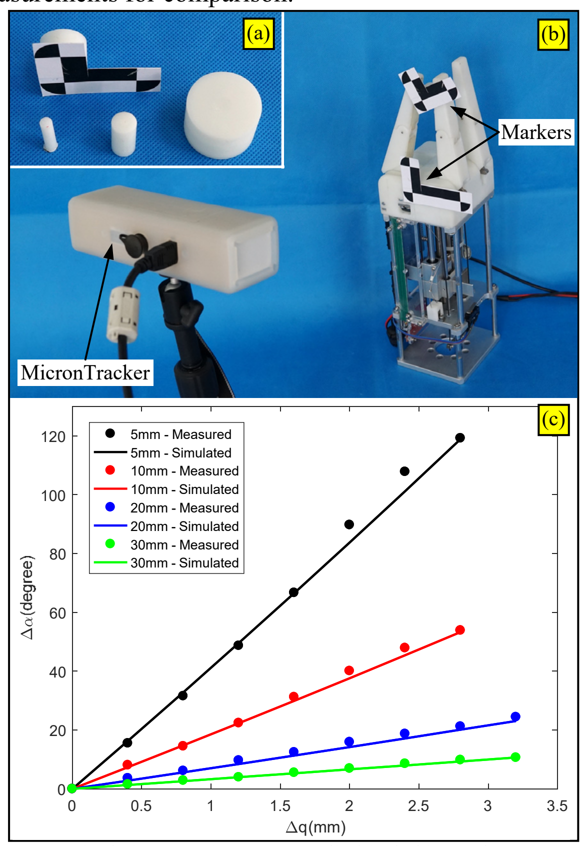

Fig. 9. Manipulation experiments: (a) cylindrical objects, (b) experimental setup, (c) simulated and measured results of rolling cylindrical objects

It can be seen from Fig. 9(c) that the measured results well matched the analysis. The absolute errors and relative errors between measured and simulated results are listed in Table II, where the relative errors are the ratios between the absolute errors and the angle ranges.

The largest absolute error is 6.62° for the Ø5 mm cylinder, while the largest relative error is 6.9% for the Ø20 mm cylinder. This result suggests that, by measuring the position of Slider-2, the configuration of the object can be well estimated, based on an initial configuration of the object.

The rolling motion range is smaller for bigger objects, since the rolling surface on the phalange is limited. This rolling manipulation may not be accurate enough for precise orientating tasks. But it can be useful for many pick-and-place tasks where a piece needs to be roughly tilted/rotated before being inserted to a packaging slot.

TABLE II. ERRORS BETWEEN SIMULATED AND MESURED RESULTS

Diameter (mm)	Measured rolling range (°)	Absolute error (°)	Relative error (%)
5	119.0	6.62	5.6
10	53.6	2.50	4.7
20	24.5	1.69	6.9
30	10.6	0.62	5.8

V. CONCLUSIONS AND FUTURE WORK

This paper presents the design, the construction and the experimentation of a single-actuator three-fingered gripper with a working mode switching mechanism for both grasping and rolling manipulation tasks. The gripper can grasp various daily-life objects in the grasping mode and can roll objects in the manipulation mode in a controllable way. The gripper may become a viable solution for reorienting the picked objects if used with a pick-and-place robot.

Future efforts will first be directed to a more general formulation of the rolling manipulation so as to extend the rolling model for non-cylindrical objects. It is also expected that the represented gripper design can inspire more design paradigms with differential motions using the simple continuum differential mechanism.

REFERENCES

[1] K. Nagata, "Manipulation by a parallel-jaw gripper having a turntable at each fingertip," in *Proceedings of the 1994 IEEE International Conference on Robotics and Automation*, 1994, pp. 1663-1670 vol.2.

[2] H. Terasaki and T. Hasegawa, "Motion planning of intelligent manipulation by a parallel two-fingered gripper equipped with a simple rotating mechanism," *IEEE Transactions on Robotics and Automation,* vol. 14, pp. 207-219, 1998.

[3] A. Bicchi and A. Marigo, "Dexterous Grippers: Putting Nonholonomy to Work for Fine Manipulation," *The International Journal of Robotics Research,* vol. 21, pp. 427-442, 2002.

[4] V. Tincani, M. G. Catalano, E. Farnioli, M. Garabini, G. Grioli, G. Fanton*, et al.*, "Velvet fingers: A dexterous gripper with active surfaces," in *2012 IEEE/RSJ International Conference on Intelligent Robots and Systems*, 2012, pp. 1257-1263.

[5] F. Chen, C. Luca, C. Carlo, D. I. Mariapaola, and C. Ferdinando, "Design of a Novel Dexterous Robotic Gripper for In-hand Twisting and Positioning Within Assembly Automation," *Assembly Automation,* vol. 35, pp. 259-268, 2015.

[6] N. Rahman, L. Carbonari, M. D'Imperio, C. Canali, D. G. Caldwell, and a. F. Cannella, "A dexterous gripper for in-hand manipulation," in *2016 IEEE International Conference on Advanced Intelligent Mechatronics (AIM)*, 2016, pp. 377-382.

[7] N. C. Dafle, A. Rodriguez, R. Paolini, B. Tang, S. S. Srinivasa, M. Erdmann*, et al.*, "Extrinsic dexterity: In-hand manipulation with external forces," in *2014 IEEE International Conference on Robotics and Automation (ICRA)*, 2014, pp. 1578-1585.

[8] N. C. Dafle and A. Rodriguez, "Prehensile pushing: In-hand manipulation with push-primitives," in *2015 IEEE/RSJ International Conference on Intelligent Robots and Systems (IROS)*, 2015, pp. 6215-6222.

[9] F. E. Vina, Y. Karayiannidis, K. Pauwels, C. Smith, and D. Kragic, "In-hand manipulation using gravity and controlled slip," in *2015 IEEE/RSJ International Conference on Intelligent Robots and Systems (IROS)*, 2015, pp. 5636-5641.

[10] J. Shi, J. Z. Woodruff, Paul B. Umbanhowar, and K. M. Lynch, "Dynamic In-Hand Sliding Manipulation," *IEEE Transactions on Robotics,* vol. 33, pp. 778-795, 2017.

[11] L. U. Odhner and A. M. Dollar, "Stable, open-loop precision manipulation with underactuated hands," *The International Journal of Robotics Research,* pp. 1347-1360, 2015.

[12] L. U. Odhner, L. P.Jentoft, M. R. Claffee, N. Corson, Y. Tenzer, R. R. Ma*, et al.*, "A compliant, underactuated hand for robust manipulation," *The International Journal of Robotics Research,* vol. 33, pp. 736-752, 2014.

[13] N. Rojas, R. R. Ma, and A. M. Dollar, "The GR2 Gripper: An Underactuated Hand for Open-Loop In-Hand Planar Manipulation," *IEEE Transactions on Robotics,* vol. 32, pp. 763-770, 2016.

[14] B. Ward-Cherrier, N. Rojas, and N. F. Lepora, "Model-Free Precise in-Hand Manipulation with a 3D-Printed Tactile Gripper," *IEEE Robotics and Automation Letters,* vol. 2, pp. 2056-2063, 2017.

[15] R. R. Ma, W. G. Bircher, and A. M. Dollar, "Toward robust, whole-hand caging manipulation with underactuated hands," in *2017 IEEE International Conference on Robotics and Automation (ICRA)*, 2017, pp. 1336-1342.

[16] H. v. Hoof, T. Hermans, G. Neumann, and J. Peters, "Learning robot in-hand manipulation with tactile features," in *2015 IEEE-RAS 15th International Conference on Humanoid Robots (Humanoids)*, 2015, pp. 121-127.

[17] K. Xu and H. Liu, "Continuum Differential Mechanisms and Their Applications in Gripper Designs," *IEEE Transactions on Robotics,* vol. 32, pp. 754-762, 2016.

[18] L. Birglen and C. M. Gosselin, "Kinetostatic Analysis of Underactuated Fingers," *Robotics and Automation, IEEE Transactions on,* vol. 20, pp. 211-221, 2004.

[19] L. Birglen and C. M. Gosselin, "Force Analysis of Connected Differential Mechanisms: Application to Grasping," *The International Journal of Robotics Research,* vol. 25, pp. 1033-1046, 2006.

[20] C. Gosselin, F. Pelletier, and T. Laliberte, "An Anthropomorphic Underactuated Robotic Hand with 15 Dofs and a Single Actuator," in *Robotics and Automation, 2008. ICRA 2008. IEEE International Conference on*, 2008, pp. 749-754.

[21] N. Fukaya, S. Toyama, T. Asfour, and R. Dillmann, "Design of the TUAT/Karlsruhe Humanoid Hand," in *Intelligent Robots and Systems, 2000.(IROS 2000). Proceedings. 2000 IEEE/RSJ International Conference on*, 2000, pp. 1754-1759.

[22] L. Birglen, C. Gosselin, and T. Laliberté, *Underactuated Robotic Hands* vol. 40: Springer, 2008.

[23] V. Begoc, S. Krut, E. Dombre, C. Durand, and F. Pierrot, "Mechanical design of a new pneumatically driven underactuated hand," in *Robotics and Automation, 2007 IEEE International Conference on*, 2007, pp. 927-933.

[24] K. Xu, H. Liu, Z. Liu, Y. Du, and X. Zhu, "A Single-Actuator Prosthetic Hand Using a Continuum Differential Mechanism," in *IEEE International Conference on Robotics and Automation (ICRA)*, Seattle, Washington, USA, 2015, pp. 6457-6462.

[25] B. Calli, A. Walsman, A. Singh, S. Srinivasa, P. Abbeel, and A. M. Dollar, "Benchmarking in Manipulation Research: Using the Yale-CMU-Berkeley Object and Model Set," *IEEE Robotics & Automation Magazine,* vol. 22, pp. 36-52, 2015.